PROCEEDINGS OF SPIE

SPIEDigitalLibrary.org/conference-proceedings-of-spie

Measuring material thickness variations through tri-aperture DSPI

Estiven Sánchez Barrera, Joao Luis Ealo Cuello

Estiven Sánchez Barrera, Joao Luis Ealo Cuello, "Measuring material thickness variations through tri-aperture DSPI," Proc. SPIE 12524, Dimensional Optical Metrology and Inspection for Practical Applications XII , 125240C (15 June 2023); doi: 10.1117/12.2663667

SPIE.

Event: SPIE Defense + Commercial Sensing, 2023, Orlando, Florida, United States

Measuring Material Thickness Variations Through Tri-Aperture DSPI

Estiven Sánchez Barrera*[a,b], Joao Luis Ealo Cuello[b]

[a]Faculty of Basic Sciences, Universidad Tecnológica de Bolívar, Cartagena Colombia
[b]Vibrations and Acoustics Laboratory, School of Mechanical Engineering, Universidad del Valle, Cali Colombia.

ABSTRACT

A configuration for the measurement of thickness changes in materials through one-shot digital speckle pattern interferometry (DSPI) was developed. The phase maps calculation was made by adding carrier fringes by the multiple aperture principle and Fourier Transform Method (FTM). With this setup, interferometry configurations verified that the simultaneous and instantaneous visualization of two opposite faces of a surface is possible. In addition, the combination of the simultaneous results obtained from both sides of the material makes it possible to determine displacements with greater sensitivity or to identify changes in their thickness. The validation and demonstrative tests were carried out with a *1 mm* thick aluminum plate with a *5 mm* diameter through hole coated. Thickness changes until *2 μm* was measured.

Keywords: DSPI, Carrier Fringes, Fourier Transform Method, Multiple Aperture, Thickness Variations.

1. INTRODUCTION

Digital Speckle Pattern Interferometry (DSPI) is a widely used interferometric technique for the measurement of displacements on the surface of an object under analysis[1]. After receiving the application of an external excitation, responsible for provoking the necessary effects for the inspection, the images of the surface deformation fields are obtained and represented by combining the calculation of phase maps and interferometry techniques.[2]

In the conventional implementation of the technique, the phase calculation is performed using the Temporal Phase method Measurement (TPM), in which the acquisition of at least three interference images with known phase shifts between them is required[3]. With the set of images, the phase values in each pixel of the image are obtained, resulting in a matrix with the phase information, known as a phase map[4]. Two different phase maps are calculated before and after applying the excitation to the test material, and their difference leads to the measurement result. One of the difficulties of the TPM technique is that images are acquired at different instants of time, so it is not appropriate for dynamic measurements or when the sample surface suffers important changes between acquisitions. In addition, TPM experimental configuration requires an element that causes the phase shifting of the images, which makes additional electronics necessary for the camera and the lighting system.[2] To circumvent this difficulty, techniques such as Spatial Phase Measurement (SPM) are the most suitable.[5] Of the SPM techniques, two types of approaches are best known. In one of them, a pixelated mask is employed to produce a particular phase shift distribution between neighboring pixels.[6] This implementation has the difficulty of being expensive since a microfabricated element must be aligned pixel by pixel with the sensor of the camera used. In the second one, a carrier frequency is added, resulting in images known as carrier fringes, which are then processed by employing the Fourier Transform Method (FTM).[7] As a result, the processing of the phase maps is accomplished using just a single image for each excited state. The main advantage of this technique is that the carrier frequency can be added by means of small differences in the optical paths, the simplest way being the addition of masks with different apertures.[8] This allows the system to

Further author information:
E.S.B.: E-mail: barrerae@utb.edu.co

Dimensional Optical Metrology and Inspection for Practical Applications XII, edited by Kevin G. Harding, Song Zhang, Jae-Sang Hyun, Proc. of SPIE Vol. 12524, 125240C · © 2023 SPIE · 0277-786X · doi: 10.1117/12.2663667

be cheaper and easier to implement. In contrast, its main drawback is that when performing filters in the frequency plane, the effective resolution is reduced, which can be sorted out by using high-resolution cameras.

Recent work has been reported regarding the improvement of DSPI measurement with SPM. Barrera et al.[9] developed a device for lateral displacement DSPI, also known as shearography, whose objective is to perform dynamic measurement of the strain field from images with three different directions of lateral displacement, simultaneously. For this, a set of three apertures was used, which induce the formation of carrier fringes in different directions, along with three prisms, to induce lateral displacement. As a result, interferograms with sensitivity in three directions are obtained. The main advantage of this implementation is that only two images are needed, a single image for each excited state, to obtain three shearography results with lateral displacements in different directions. Obtaining interference fringes from two images creates the concept of simultaneous shearography.

Although it is possible to determine displacements or deformations using these different configurations, both outside and in the plane, none of them has been proposed for the identification of possible changes in the thickness of a sample material. In this work, a DSPI configuration with SPM is put forward for the simultaneous measurement of the displacement, out of the plane, of opposite faces of a laminar sample. This allows us to determine the changes in thickness in a material after applying a stimulus.[10]

2. FOURIER TRANSFORM METHOD

Fringe pattern analysis by the Fourier Transform Method (FTM) was developed by Takeda et al.[7] All the information needed for phase recovery can be simultaneously encoded in a single image, allowing analysis of transient events. The method requires the presence of carrier fringes generally formed by a set of parallel high-frequency fringes. The carrier fringe frequency can be subsequently removed in different ways. The intensity distribution in an interferogram with a carrier frequency $2\pi f_c(x)$ can be written in the form

$$I_0(x,y) = I_b(x,y) + I_m(x,y)\cos(\phi_i(x,y) + 2\pi f_c(x)), \tag{1}$$

where I_b is the background intensity, I_m is the modulation intensity, and ϕ_i is the value of the unknown phase of the speckle, all of these in terms of the image coordinates (x, y).

Applying a two-dimensional Fourier transform to the interferogram, it can be written as:

$$\mathcal{F}\{I_0(x,y)\} = A(f_x, f_y) + C(f_x - f_c, f_y) + C^*(f_x + f_c, f_y), \tag{2}$$

The resulting frequency spectrum contains three maximum regions, in the two-dimensional Fourier transform images known as halos, as shown in figure 1. The zero-frequency located in the central halo of the spectrum is the amplitude A. The desired information is present in the left and right halos $C(f_x - f_c, f_y)$ and $C^*(f_x + f_c, f_y)$, where f_x , f_y are the frequencies relative to the phase $\phi_i(x,y)$. Since the terms C and C^* are symmetric, a band-pass window filter is used around the carrier frequency to keep only the frequencies contained in the halo C. Applying the inverse Fourier transform, it is possible to obtain the complex signal $c(x,y)$[7], from which the phase can be extracted as follows:

$$\begin{aligned} \Phi(x,y) &= arctan\frac{Im[c(x,y)]}{Re[c(x,y)]} \\ &= \phi_i(x,y) + 2\pi f_c(x) \end{aligned} \tag{3}$$

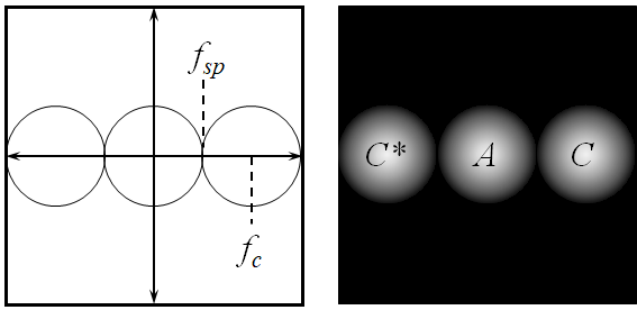

Figure 1. Representation of the bidimensional Fourier transform images with a carrier. On the left, is a representation of the axes and carrier frequency. On the right is a simulated representation of the two-dimensional Fourier transform, representing the intensity halo A and the frequency components C and the conjugate C^*.[10]

1.1 Double Aperture principle

The double aperture principle in interferometry was proposed by Bhaduri[11]. This allows to add a carrier frequency to a speckle image.

The addition of a double aperture generates carrier fringes due to the interference principle, as in Young's double-slit experiment[12], depicted in figure 2.

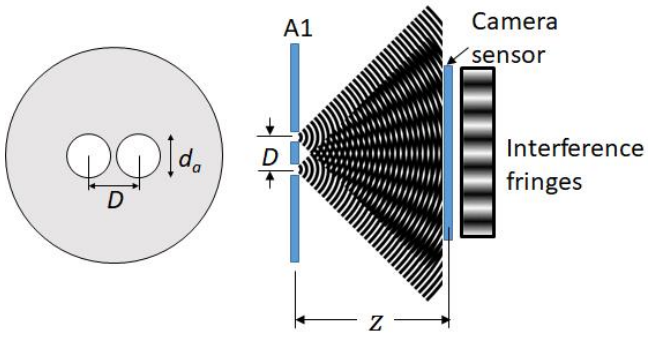

Figure 2. Formation of carrier fringes by the principle of double aperture. Left: front view of the double aperture, where the distance between apertures D and the aperture diameter da are represented. Right: effect of interference due to the difference in optical paths, caused by the distance between apertures and the distance to the camera sensor.[10]

When a coherent light passes through both apertures, the images of the two apertures are superimposed and, due to the path differences, a periodic structure is produced within each speckle image. The interference lines are perpendicular to the orientation of the apertures. The distance h, between maxima or minima, of the carrier fringes will be determined by the distance z from the aperture to the camera sensor, the wavelength λ, and the distance between apertures D, in the form:

$$h = \frac{\lambda z}{D} \tag{4}$$

Adding a carrier frequency implies that a halo separation will appear in the plane of frequencies, where, in this case, the frequency f_c corresponds to the frequency introduced by the distance between the apertures and f_{sp} is the frequency product of the size of the speckle.

3. FACE-TO-FACE SETUP

The configuration of the optical system, presented in Figure 3, allows the interference of the images acquired simultaneously from the two faces of the sample to be inspected.

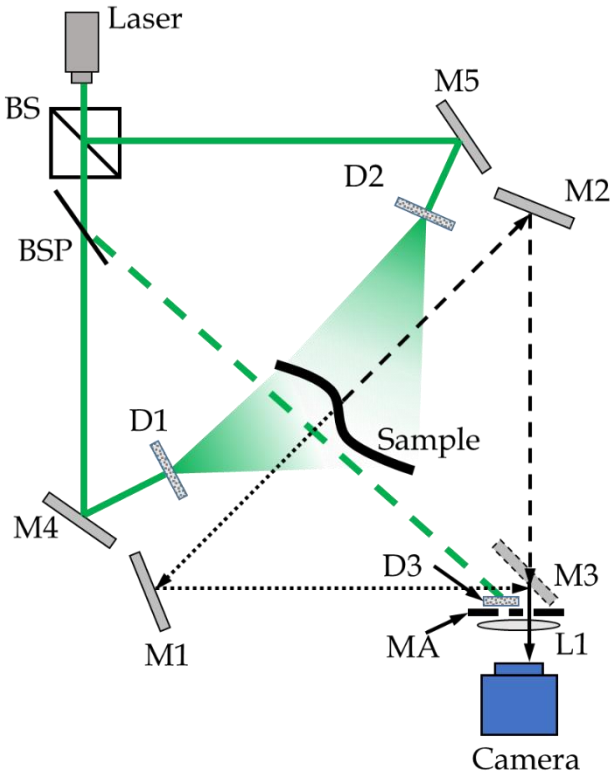

Figure 3. Optical configuration for Double-Face interferometry. **M1-M5,** Mirrors. **L1,** Image Lens. **BS,** Beamsplitter. **BSP**, Beamsplitter Plate. MA**,** Apertures Mask with horizontal and vertical orientation respectively. **D1-D3** Diffusers. The interferometer arm, with the dashed line, is oriented in the vertical direction.[10]

The illumination module is composed of a laser diode woes emitted light is divided into two paths using the beamsplitter **BS**. Each beam is reflected by the mirrors **M4** and **M5,** respectively, to later be expanded employing the diffusers **D1** and **D2**, a 90:10 factor beamsplitter plate (**BSP**) is in one of the beams. The reflection, outlined with the dashed line, is oriented to one of the apertures of the mask **MA** and then expanded using the diffuser **D3** to act as a reference beam.

The acquisition module is made up of mirrors **M1** and **M2**, which allow the sample to be viewed from both sides simultaneously. The **L1** lens contributes to the formation of the image on the camera sensor. The aperture's mask **MA** allows to control the size of the speckle and to add the carrier fringes, by properly setting the distance and orientation of the apertures. The **MA** mask is made up of three apertures, with a perpendicular configuration between them, as shown in figure 4. The aperture **A1** is aligned with the diffuser **D3**, in such a way that only the illumination of the speckle generated by the diffuser passes through this aperture and serves as a reference. The aperture **A2** is aligned with the mirror **M2**, so that the light beams passing through this aperture allow the formation of the image of a single face of the sample. The aperture **A3** is aligned with the mirror **M3** in such a way that the beams that pass through this aperture are those coming from the opposite face of the sample and were reflected by **M1** and **M3**. At the end, the image capture is done with a Basler camera Ace model acA4024-29um with a Pixel size of 1.85 $\mu m \times 1.85\ \mu m$ and the image capture routine and the image processing were done with an algorithm developed in Python.

Therefore, in this configuration, three different interferences with different carrier fringes orientations between them are obtained.

The combination of the apertures **A1** and **A2** leads to the interference of the front face of the sample with a reference beam and, due to the apertures orientation, generates vertical carrier fringes, represented in the Fourier domain as the halo A_{12} and his conjugate form A_{12}^{*}, shown in figure 4b. The interference between a beam coming from a face of the sample and a reference beam allows the out-of-plane displacements to be extracted[11], as shows in Figure 6b. The combination of apertures **A1** and **A3** generates diagonal fringes with an inclination of 45°, which leads to the interference of the rear face of the measurement sample with the reference beam, allowing the out-of-plane displacement component to be extracted. Finally, the interference between the apertures **A2** and **A3**, leads to the interference of the faces of the sample, allowing the visualization of the subtraction of the displacements of both surfaces, Figure 4b. The image of the interference from the three apertures is recorder simultaneously with a 12 bit pixel depth.

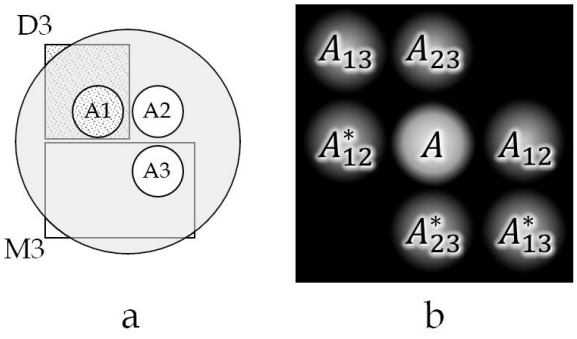

Figure 4. **a** Front view of the Aperture Mask, showing the position of the apertures **A1**, **A2,** and **A3**, and the alignment of the diffuser **D3** and the mirror **M3** with the apertures **A1** and **A3**. **b** 2D Fourier Transform simulation for the combination of apertures, **A12** stands for the combination of the apertures **A1** and **A2,** equivalent to the out-of-plane front displacement. **A13** contains the out-of-plane displacement of the back view and **A23** includes the interference of the faces of the sample. [10]

4. RESULTS

The schematic of the optical configuration was presented in figure 3. The focal length of the lens **L1** was *30 mm* and the aperture mask **MA** was placed at the same distance from the camera sensor. The configuration of the mask is the same as that presented in figure 4. The diameter was calculated to achieve a speckle size of *6 pixels*. A Basler camera Ace model acA4024-29um was used to capture the interference images. The laser used in this application was a *532nm* with power < *50mW* DPSS laser. Simple glass plates with a rough surface were used as diffusers.

An aluminum plate of *1 mm* thick was used for the measurement surface. A *5 mm* diameter hole was made, which was then filled and sealed at both ends with paper tape, to function as a region with different properties. The test sample is visible in figure 5.

Then, the test sample was fixed and the measurements were carried out. Initially, a speckle image is taken, to which the two-dimensional Fourier transform is applied, and the phase of the reference image is calculated. Subsequently, the material is stimulated by employing heat from an incandescent lamp. Images are acquired while the sample is heated and the phase maps are calculated for each new image. Also, the corresponding reference phase map is subtracted. The resulting phase map for heating time of *2 s* is visible in Figure 6.

Figure 5. Sample for thickness variations test.

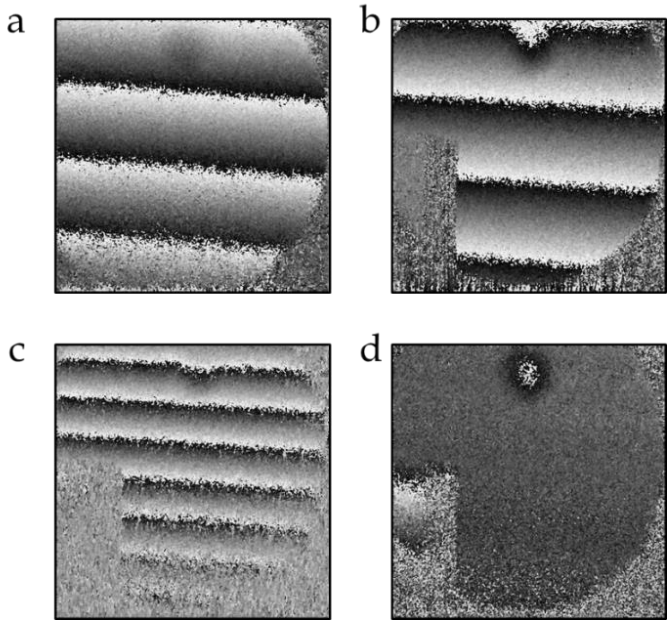

Figure 6. Deformation and result of interference images after heat stimulation of *2 s*. **a** and **b** are the interference patterns of the front and back faces respectively, **c** is their subtraction and **d** is the thickness variation distribution in radians.

In the figure 6d, the movements of the sample are eliminated and only the changes in thickness remain evident. The interference result, presented in figure 6d, was processed with a phase unwrapping algorithm and the resulting values are shown in figure 7, i.e. the distribution of thickness variation in the sample is included.

5. CONCLUSIONS

The ability to quantify changes in the thickness of the sample by simultaneously acquiring interference speckle patterns on both sides of the material has been demonstrated. The proposed configuration allows us to obtain the displacements out of the plane of each of the faces of the sample, along with the resultant thickness variations, all simultaneously. Through the addition of apertures and the FTM image processing, it was possible to calculate the phase maps for each stimulation with a single exposure. This is the equivalent of performing 4 different measurements with a single image. The proposed technique exhibits a high potential for quality control application where a rapid and precise identification of defective components is required. Further

research is being conducted in order to determine the limits of the implementation under different environmental conditions, defects, and stimulation sources.

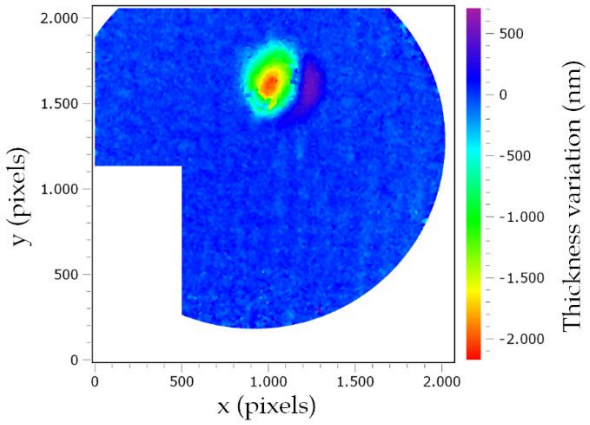

Figure 7. Thickness variation distribution of the sample after 2s of heat stimulation, obtained using the tri-aperture DSPI technique.

ACKNOWLEDGMENTS

This research was supported by the "Fondo Nacional de Financiamiento para la Ciencia, la Tecnología y la Innovación Francisco José de Caldas y la Universidad del Valle" and the "Ministerio de Ciencia y Tecnología MINCIENCIAS" [grant number 0740-750-2020].

REFERENCES

[1] M. P. Georges, C. Thizy, F. Languy, and J.-F. Vandenrijt, "An overview of interferometric metrology and NDT techniques and applications for the aerospace industry," SPIE Proceedings, Aug 2016

[2] M. R. Viotti and A. Albertazzi, Robust speckle metrology: techniques for stress analysis and NDT. Spie Press, 2014.

[3] P. de Groot, Phase Shifting Interferometry. Berlin, Heidelberg: Springer Berlin Heidelberg, 2011, pp. 167–186.

[4] J. Wyant, "Interferometry — overview," in Encyclopedia of Modern Optics, R. D. Guenther, Ed. Oxford: Elsevier, 2005, pp. 351–356.

[5] K. Creath and J. Schmit, "N-point spatial phase-measurement techniques for non-destructive testing," Optics and Lasers in Engineering, vol. 24, no. 5-6, p. 365–379, May 1996.

[6] K. Creath and G. Goldstein, "Dynamic quantitative phase imaging for biological objects using a pixelated phase mask," Biomedical Optics Express, vol. 3, no. 11, p. 2866, Oct 2012.

[7] M. Takeda, H. Ina, and S. Kobayashi, "Fourier-transform method of fringe-pattern analysis for computer-based topography and interferometry," Journal of the Optical Society of America, vol. 72, no. 1, p. 156, Jan 1982.

[8] B. Bhaduri, "Direct measurement of curvature and twist using two-channel double-aperture digital shearography," Optical Engineering, vol. 49, no. 3, p. 033604, Mar 2010.

[9] E. S. Barrera, A. V. Fantin, D. P. Willemann, M. E. Benedet, and A. Albertazzi Gonçalves Jr., "Multiple-aperture one-shot shearography for simultaneous measurements in three shearing directions," Optics and Lasers in Engineering, vol. 111, no. 0143-8166, p. 86–92, Dec 2018.

[10] E. S. Barrera, J. L. Ealo, "Measuring material thickness changes through tri-aperture digital speckle pattern interferometry," Opt. Eng. 62(1) 014108, 31 January 2023.
[11] B. Bhaduri, N. K. Mohan, M. P. Kothiyal, and R. S. Sirohi, "Use of spatial phase shifting technique in digital speckle pattern interferometry (DSPI) and Digital Shearography (DS)," Optics Express, vol. 14, no. 24, p. 11598, Nov 2006.
[12] G.-W. Chang, Y.-H. Lin, and Z.-M. Yeh, "White light interferometric profile measurement system using spectral coherence," in Reliability, Packaging, Testing, and Characterization of MEMS/MOEMS VI, A. L. Hartzell, and R. Ramesham, Eds., vol. 6463, International Society for Optics and Photonics. SPIE, 2007, pp. 164 – 174.